

## 2-D Analytic signal application in electrical profiling problems

Rambhatla G. Sastry and Mukesh Gupta<sup>1</sup>

Department of Earth Sciences, IIT, Roorkee – 247 667

<sup>1</sup>Well Log Services, ONGC Mehsana Asset, Mehsana, Gujarat

E.mail: rgss1fes@iitr.ernet.in, rgssastry@yahoo.com, mukeshgupta04@yahoo.com

---

### ABSTRACT

Our 2-D stabilized analytic signal algorithm (RESAS) is used in interpreting synthetic electrical profiling data due to 2-D resistive / conductive bodies of both closed and open geometries. For bodies of closed geometry, pole-pole profiles with buried current pole above body center are considered while for open geometries, pole-pole (Half - Wenner) / pole-dipole apparent resistivity profiles are opted for. The analytic signal parameters like, Amplitude of the Analytic Signal (AAS), Real (RIAS) and imaginary parts (IIAS) of complex analytic signal inverse are used in the analysis.

Synthetic buried pole-pole data is generated by finite-difference based resistivity modeling algorithm and this data served as input to RESAS. The numerical models included conductive bodies of closed geometry (Prism in 2-layered earth medium and two inclined dyke model) and open geometry (a faulted bed and Horst – Graben model).

Achieved results show that AAS generally meets the interpretation requirements; but analyses of RIAS and IIAS are needed either to confirm the lateral coordinates inferred by AAS or supplement such information in case AAS fails.

For body corners with same lateral coordinates (bodies with vertical dips), analytical signal method fails in segregating them and ambiguity arises. Further, numerical results confirm that profiles of sufficient length are needed to image the lower corners of anomaly causative sources. The obtained results validate the proposed interpretation procedure.

---

### INTRODUCTION

Resistivity imaging is currently utilized for tackling a wide variety of near surface geophysical problems. The state-of-art resistivity imaging algorithms either deals with improved pseudo-section concepts (Loke & Barker 1995) or computer –intensive resistivity inversions (Li & Oldenburg 1994). However, there is a practical need for simple and effective means of implementing resistivity inversion of profile data under field conditions. The current effort is devoted to this aspect.

Loke & Barker (1995) have proposed an inversion scheme for dipole-dipole pseudo-section data. The analytic expression of apparent resistivity for half space is chosen as the starting point, which is iteratively varied for building a block resistivity structure of subsurface. But the success of this approach depends on depth of investigation concepts.

Analytic Signal method (Nabighian 1972; Roest, Verhoef & Pilkington 1992) or its variants (Rao, Ram Babu & Shankar Narayan 1981; Ofoegbu & Mohan, 1990; Sunderrajan, Srinivasa Rao & Sunitha 1998) have

been proposed in the past for interpretation of potential field anomalies and S.P. anomalies. The success of analytic signal method (Nabighian 1972; Roest, Verhoef & Pilkington 1992) and the formal analogy between magnetostatics and electrostatics (Eskola 1992; Quick 1974) allow its use (Pujari 1998, Pujari & Sastry, 2003) in the analysis of DC pole-pole secondary electric potential data caused by 2-D conductive / resistive closed bodies of rectangular cross-section.

Effective complex analytic signal computation depends on getting stable numerical derivatives of either secondary pole-pole electric potentials (Pujari & Sastry 2003) for bodies with closed geometry or apparent resistivity data for bodies of both open and closed geometries. Tikhonov's regularization is incorporated in the design of stable analytic signal algorithm, RES2AS by Pujari & Sastry (2003).

Here, we have used our RESAS, an updated version of RES2AS for interpreting either pole-pole secondary potential data or electrical resistivity profiling data. For synthetic data generation, forward responses of

isolated 2D conductive/resistive bodies of either open or closed geometry enclosed within resistive/ conductive host medium are computed using Dey & Morrison's (1979) algorithm using software code by Dey (1976).

In our attempts, physical property (electrical resistivity) is not being assessed. Our estimates include the model parameters (Depth to the top surface, lateral extent etc.) through plots of various analytic signal parameters to be elaborated later.

The synthetic experiments include secondary pole-pole potential / apparent resistivity data due to 2D conductive targets of closed geometry (single prism in a two layered resistive medium and inclined two dyke model in resistive half-space) and open geometry (fault model and horst – graben model). The depth rules for interpreting Amplitude of stable Analytic Signal (AAS) plot are either based on Nabighian's (1972) or on empirical means through numerical simulations. The accrued results of numerical experiments (Mukesh, 2004) are quite encouraging for adoption of the proposed method in formulation of initial guess model(s).

### FUNDAMENTAL EQUATIONS

The flow of steady electric current in an inhomogeneous medium is governed by

$$\nabla \left[ \frac{1}{\rho(x, y, z)} \nabla v(x, y, z) \right] + \frac{\partial Q}{\partial t}(x, y, z) = 0 \quad (1)$$

where,

- $\rho$  resistivity of the medium ( $\Omega\text{-m}$ )
- $v$  potential (volts)
- $Q$  charge density ( $\text{coul.m}^{-3}$ )

We may write equation (1) as

$$\nabla[\sigma(x, y, z)\nabla v(x, y, z)] + q(x, y, z) = 0 \quad (2)$$

where,

$$\sigma(x, y, z) = \frac{1}{\rho(x, y, z)} \text{ is conductivity of the medium } (\Omega^{-1}\text{m}^{-1})$$

$$\text{and } q(x, y, z) = \frac{\partial Q(x, y, z)}{\partial t}, \text{ is current density (amp m}^{-3}\text{)}$$

### Forward Problem

Here, based on eqn. (2), the finite-difference d.c resistivity forward modeling (Dey & Morrison 1979) estimates pole-pole or pole-pole dipole potential field over an arbitrary two - dimensional conductivity / resistivity distribution in the subsurface.

### Stabilized Analytic Signal Method

The construction of analytic Signal involves numerical derivative evaluations from the input potential field data. However, such numerical derivative computations are unstable (Tikhonov & Arsenin 1977). Hence, one needs to employ a regularization strategy for evaluation of stable numerical derivatives, which in turn will lead to a stable Analytic Signal computation.

### 2-D Analytic Signal

The analytic signal is defined as a complex function whose real and imaginary parts constitute a Hilbert Transform pair.

Following Nabighian (1972), the 2-D analytical signal,  $A(X,Z)$  of the secondary pole-pole potential  $V_s(x,z)$  or apparent resistivity can be defined as

$$A(x, z) = \frac{\partial V'_s}{\partial x} + j \frac{\partial V'_s}{\partial z} \quad (3)$$

$$\text{where } j = \sqrt{-1}$$

The amplitude of the analytic signal is given by

$$|A(x, z)| = \sqrt{\left[ \frac{\partial V'_s}{\partial x} \right]^2 + \left[ \frac{\partial V'_s}{\partial z} \right]^2} \quad (4)$$

$$\text{where } V'_s = \frac{\partial V_s}{\partial x}$$

The real and imaginary parts of R.H.S. of eqn. (3) constitute a Hilbert Transform pair (Nabighian 1972). In view of numerical derivative computations being unstable (Tikhonov & Arsenin 1977), analytic signal computation is an ill-posed problem. So, our spectral algorithm (RESAS), an updated version of Pujari & Sastry (2003) uses both regularization strategy (Tikhonov & Arsenin 1977) and FFT routines. In RESAS a more effective FFT routine from Press et al. (1994) is used and the rest of the logic remain unchanged.

The computation of  $n^{\text{th}}$  order derivative of a given arbitrary function  $u(x)$  is governed by Volterra type Integral equation (Tikhonov & Arsenin 1977) of first kind of convolution type given by

$$\int_0^t \frac{1}{(n-1)!} (t-\xi)^{(n-1)} z(\xi) d\xi = u(t) \quad (5)$$

which is ill-posed.

In operator form, eqn. (5) can be written as

$$Az = u \tag{6}$$

where

$z \in Z, u \in U$  with  $Z$  and  $U$  as Hilbert spaces.

In Fourier domain, the spectrum of  $z(t)$  is given by

$$\tilde{Z}(\omega) = \frac{\tilde{U}(\omega)}{\tilde{K}(\omega)} \tag{7}$$

Where the Fourier transform pairs are

$$\begin{aligned} k(t) &\Leftrightarrow \tilde{K}(\omega) \\ z(t) &\Leftrightarrow \tilde{Z}(\omega) \\ u(t) &\Leftrightarrow \tilde{U}(\omega) \end{aligned} \tag{8}$$

and  $\omega$ , is the spatial frequency and  $k(t)$ , the kernel of (5).

However, in view of ill- posedness of (5), Inverse Fourier Transform, IFFT of (7) does not exist.

Then, the regularised solution as per Tikhonov & Arsenin (1977) is given by

$$Z_{\alpha}(t) = IFFT\left(\frac{\tilde{u}(\omega)}{\tilde{k}(\omega)} f(\omega, \alpha)\right) \tag{9}$$

where  $\omega$  and  $\alpha$  are respectively spatial frequency and parameter of regularization.

The spectral function,  $f(\omega, \alpha)$  is defined to be

$$f(\omega, \alpha) = \frac{1}{\{1 + \alpha\omega^{2p}\}} \tag{10}$$

where  $p$ , order of regularization

Here, we have chosen  $\alpha = 0.1$  and  $p=2$ .

### INPUT DATA PREPARATION

The charge accumulation concepts of Li & Oldenburg (1991) stress the need of secondary potential estimation in resistivity profile interpretations for conductive / resistive targets of closed geometry.

In case of isolated closed bodies located within a layered medium, secondary potential is calculated by subtracting the layered half space potential from observed total potential i.e.,

$$V^s(s) = V^t(x) - V^l(x) \tag{6}$$

Where,

- $V^s(x)$  secondary potential
- $V^t(x)$  total potential
- $V^l(x)$  layered space potential

### Analytic Signal Parameters

Nabighian (1972) has identified the following properties of complex Analytic Signal of magnetic

anomaly due to a 2-D body of arbitrary cross-section, approximated by an  $n$ -sided polygon.

a) The amplitude of analytic signal, AAS is a symmetrical function maximizing exactly over the top of each corner of 2-D body.

b) The complex analytic signal, AS has simple poles at each corner of the arbitrary shaped 2-D body and conversely,  $1/A(x,z)$  has zeros at those corners. So, the real part of inverse of AS is zero at the body corner.

Thus the AAS can be used for computing the depth to top of the body and poles of AS fix the lateral edges of the body.

The various AS parameters relevant for interpretation are

- a) Amplitude of Analytic Signal (AAS).
- b) Real part of  $1/A(x, z)$  i.e., (RIAS).
- c) Imaginary part of  $1/A(x, z)$  i.e., (IIAS).

The AAS is used for defining body corners (both depth and lateral coordinates). However, for confirmation of lateral coordinates or when AAS fails RIAS and IIAS, revealing the zeros of the inverse of analytic signal (AS), are used. Here, we use both AAS and RIAS plots for interpretation.

We found from synthetic models that there is no need of secondary potential generation due to bodies of open geometry and one can directly work with apparent resistivity data itself.

### Depth Rules

Nabighian's (1972) depth rule for a single corner is adapted for bodies of closed geometry, which refers to depth  $d = x_{1/2}$ . For bodies of open geometry, empirically depth rules are designed on the basis of numerical experiments. Further, the depth  $d=2x_{1/2}$  can be adopted for bodies of open geometry.

### RESULTS AND DISCUSSION

#### Case I (Bodies of Closed geometry)

For geological models of closed geometry, synthetic secondary pole-pole potential data is generated by Dey and Morrison's (1979) algorithm, RES2D and interpreted through our RESAS algorithm

#### Single Vertical Conductive Prism in Layered Medium

Input model for single conductive prism in layered medium is shown in Fig.1a. Source is located (36, -1) above the body center of Prism. Depth of current source is 1m. below air-earth interface. The computed secondary pole-pole potential along principal profile is

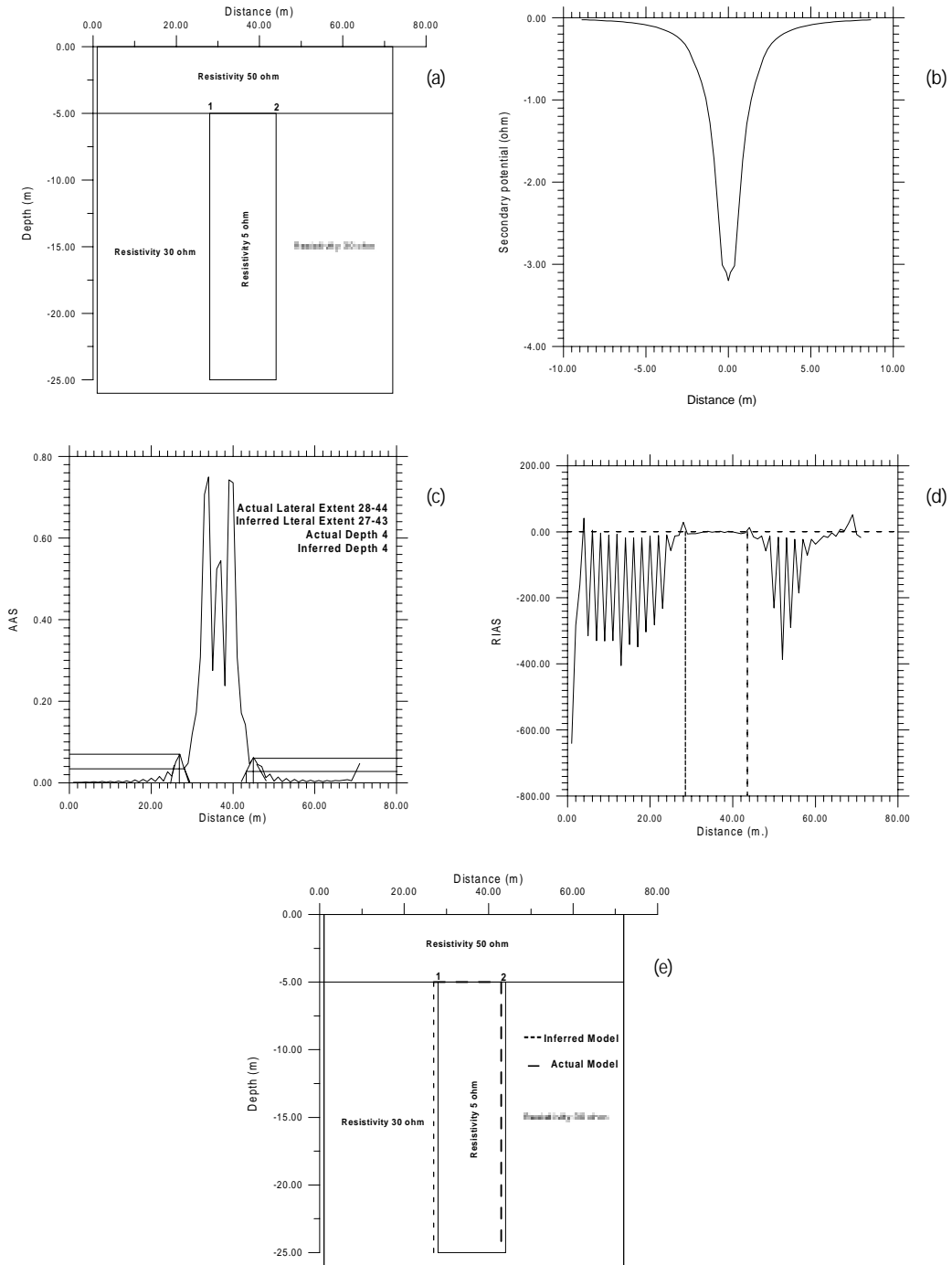


Figure 1a). Single vertical prism of resistivity 5 ohm-m embedded within a two – layered earth medium. The layer resistivities are respectively 50 and 30 ohm-m respectively. Top corners of prism are marked as 1 and 2. Depths are indicated with negative values. b) Secondary pole-pole potential profile for a buried current pole 4m above the body center of prism and 1m below air-earth interface. Distance in meters is plotted along X-axis. c) Amplitude of Analytic Signal (AAS) profile for prism model (Fig. 1a). The inferred lateral extent and depth of 2D – prism are compared with actual ones. Only top corners of prism (1 and 2 corners in Fig. 1a) could be identified due to superposition of analytic signals arising from bottom corners. d) Real component of complex inverse Analytic Signal (RIAS) profile for prism model (Fig. 1a). Zero crossings of RIAS identify the top corners (1 and 2 in Fig. 1a) of the prism. e) Inter - comparison of Inferred (broken line) and actual models. Here AAS plot (Fig. 1c) results are used. Depths are indicated with negative values.

Table 1. Results of Stabilized Analytic Signal (AS) Algorithm for Vertical Prism Model (Figs.1a, 1e)

Estimation of Lateral and depth* coordinates (X,Z) of body corners by RESAS.			
Top Body Corners	RIAS (X- Coordinate) (m.)	AAS ((X,Z) Coordinates) (m.)	Actual Coordinates of body corners ((X,Z) Coordinates) (m.)
Fig. 1a	Fig. 1d	Fig. 1c	Fig. 1a
1	28	(27,4)	(28,4)
2	44	(43,4)	(44,4)

\* Depth estimates refer to depths of body corners below electrode configuration level. Buried pole -pole configuration is 1m below air-earth interface and above body center.

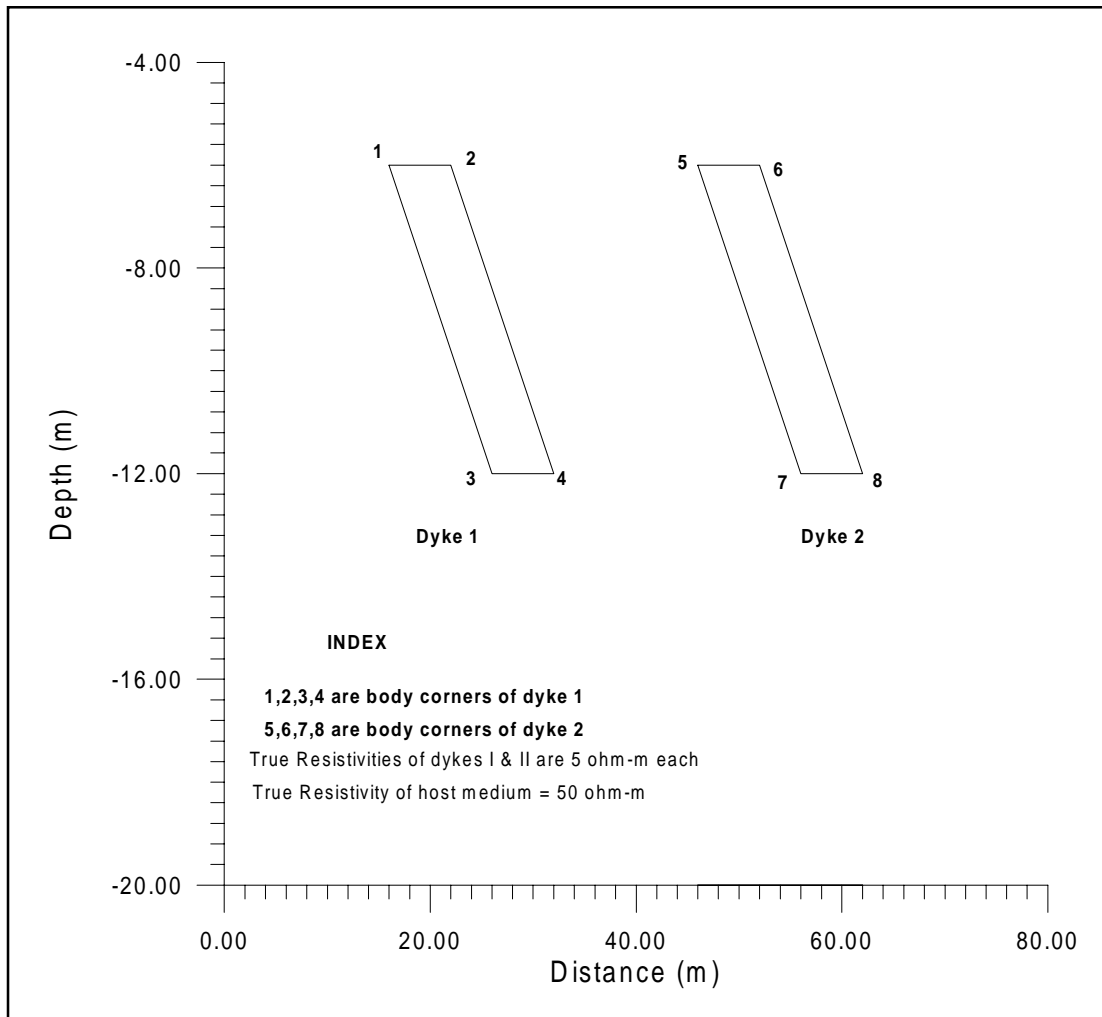


Figure 2. Two inclined conductive dykes of resistivity 50ohm-m each within homogeneous half-space of resistivity 50 ohm-m. Corners 1, 2, 3 and 4 refer to Dyke 1 and 5,6,7 and 8 to Dyke 2.

displayed in Fig.1b and this data formed input to our RESAS. The output of RESAS yielded AAS (Fig.1c) and RIAS (Fig.1d). As per earlier outlined methodology, both AAS and RIAS plots are interpreted and the summary is tabulated in Table 1 and also in Fig. 1e. Both Table 1 and Fig.1e reveal that AAS plot has got better interpretative value than RIAS plot.

Conductive Double Dyke Model

Two inclined dykes (prisms) in halfspace are shown in Fig.2. The objective would be to assess body

corners of first (1,2,3,4) and second dykes (5,6,7,8) by an analysis based on RESAS.

Buried current pole above center of Dyke 1

Input data using RES2D is generated for current source location (22, -1) just above the center of first prism. Depth of the current source is 1 m. below air-earth interface. Secondary potential is determined by removing the effect of host medium, and the principle profile considered across the strike of body is plotted.

Secondary potential data (Fig. 3a) is used as an

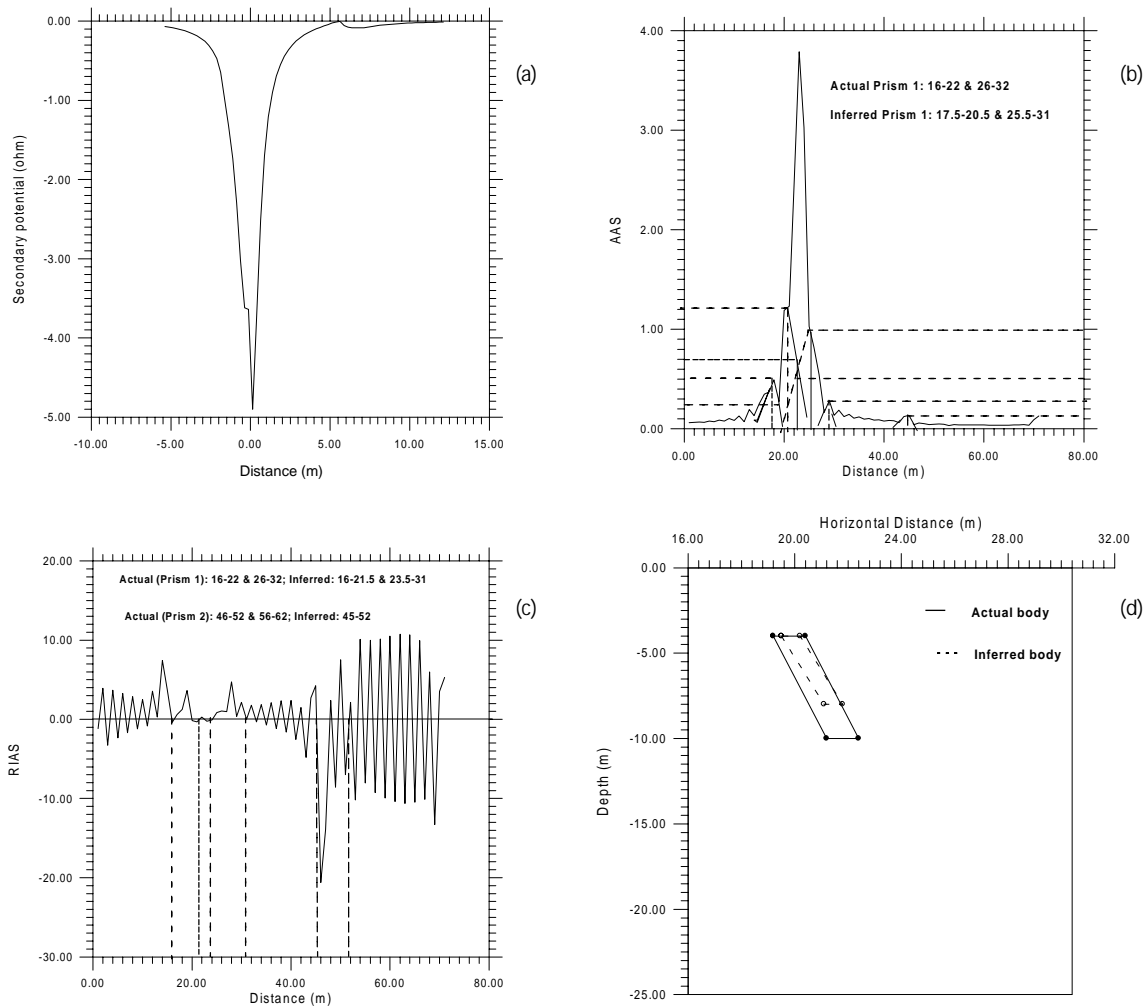


Figure 3a). Secondary pole-pole potential profile for Dyke 1 (Prism 1) in Fig. 2 due to a buried point source at 4m above prism’s body center. This point source pole’s depth is 2m below air-earth interface. Distance in meters is plotted along X-axis. b) Amplitude of Analytic Signal (AAS) profile for Dyke 1 in Fig.2. Inferred coordinates (m) for corners 1, 2, 3 and 4 of Dyke 1 are respectively (17.5, 4), (20.5, 4), (25.5, 8) and (31, 8) as against its true coordinates (16, 4), (22, 4), (26, 10) and (32, 10). c) Real component of complex inverse Analytic Signal (RIAS) profile for Prism 1. RIAS zero crossings infer the lateral edges of the body. Both actual (Fig. 2) and inferred lateral coordinates of corners 1, 2, 3 and 4 of Dyke1 are compared. d) Interpretation result for Dyke 1. Both actual (bold line) and inferred (dashed line) models are presented. Here inferred depth values refer dyke’s location below pole – pole configuration. Depths are indicated with negative values.

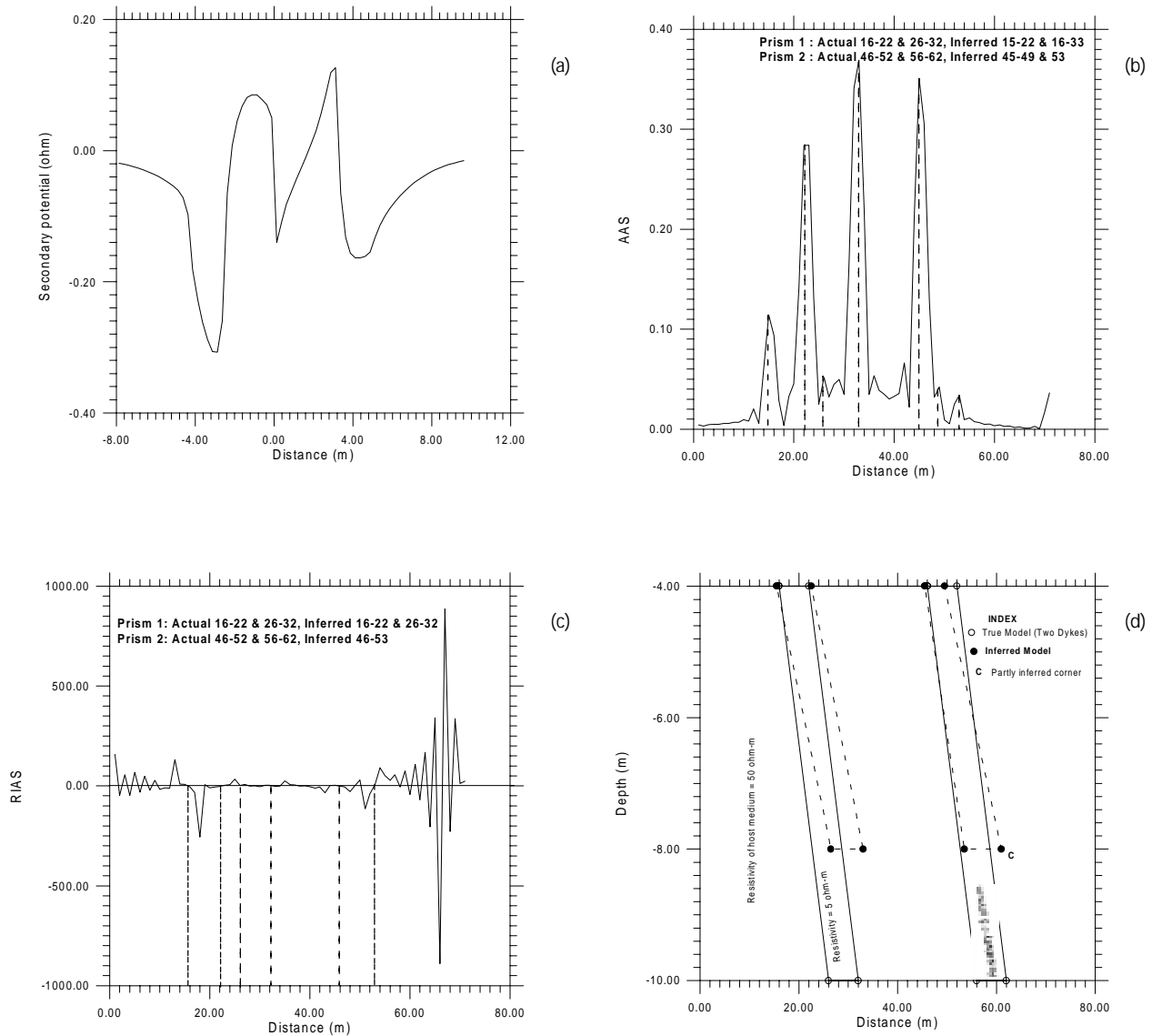


Figure 4a). Secondary pole-pole potential profile for a Double Dyke model (Fig. 2) with a buried current pole located mid-way of body centers. The emplacement depths of buried current pole with respect to air-earth interface and dyke are respectively 2m and 4m. For this fixed current pole, the potential pole is emplaced at same depth at various stations along principal profile to get total potential profile. b) Amplitude of Analytic Signal (AAS) profile for Double Dyke (Prism) (Fig. 4a). Inferred coordinates in meters for corners of Dyke 1 and Dyke 2 (Fig. 2) are respectively 1(15, 4), 2(22,4), 3(26, 8), 4(33, 8), 5(45, 4), 6(49, 4), 7(53, 8) against true coordinates 1(16,4), 2(22, 4), 3(46, 10), 4(52, 10), 5(26, 4), 6(32, 4), 7(56, 10) and 8(62, 10). Corner 8 of Dyke 2 could not be inferred. c) Real component of complex inverse Analytic Signal (RIAS) profile for Double Dyke (Fig.2). RIAS zero crossings infer the lateral edges of the dykes. Both actual (Fig. 2) and inferred lateral coordinates of corners of dykes (prisms) are compared. d) Interpretation result for Double Dyke (Prim) model (Fig. 2). Both actual (bold line) and inferred (dashed line) models are presented. Here indicated depths refer to buried electrode configuration's depth level. Here, in addition to AAS results (Fig. 4b), RIAS results for corner 8 of Dyke 2 (Fig. 2) are used. Further, the depth of corner 8 is assumed to be same as that of corner 7 (Fig. 2). Depths are indicated with negative values.

Table 2. Results of Stabilized Analytic Signal (AS) Algorithm for Dyke 1 of Double Dyke Model (Figs. 2, 3d)

Interpretation using RESAS (Dyke 1) Estimation of Lateral and depth* coordinates (X,Z) of body corners.			
Body Corner	RIAS (X- Coordinate) (m.)	AAS ((X,Z) Coordinates) (m.)	Actual Coordinates of body corners (X,Z) Coordinates) (m.)
Fig. 2	Fig. 3c	Fig. 3b	Figs. 2 &3d
1	16	(17.5,4)	(16,4)
2	21.5	(20.5,4)	(22,4)
3	23.5	(25.5,8)	(26,10)
4	31	(31,8)	(32,10)

\* Depth estimates refer to depths of body corners below electrode configuration. The depth of buried pole - pole configuration is 2m below air-earth interface.

Table 3. Results for double dyke model using RESAS (Figs. 2, 4d)

Interpretation for Dyke 1 Estimation of Lateral and depth* coordinates (X, Z) of body corners.			
Body Corner	RIAS (X- Coordinate) (m.)	AAS ((X, Z) Coordinates) (m.)	Actual Coordinates of body corners (m.)
Fig. 2	Fig. 4c	Fig. 4b	Fig. 2
1	16	(15.5,4)	(16,4)
2	22	(22.5,4)	(22,4)
3	26	(26.5,8)	(26,10)
4	32	(33,8)	(32,10)
Interpretation for Dyke 2			
5	46	(45.5,4)	(46,4)
6	53	(49.5,4)	(52,4)
7	23.5	(53.5,8)	(56,10)
8	61	-	(62,10)

\* Depth estimates refer to depths of body corners below electrode configuration level. Buried pole - pole configuration is 2m below air-earth interface with fixed current pole occurring midway between body centers.

input for RESAS and the resulting AAS (Fig. 3b) and RIAS (Fig.3c) are interpreted to locate body corners of Dyke I.

Using Fig. 3d, the parameters of Prism 1 are established and are summarized in Table 2. Depth estimates are with reference to buried current source position, i.e., 2m. below air-earth interface.

Buried current source midway between body centers of both dykes at 2m below air-earth interface

Input data using RES2D is generated for current source location (32, -1) just above the first prism. Depth of the current source is 1 m. from air-earth interface.

## 2-D Analytic signal application in electrical profiling problems

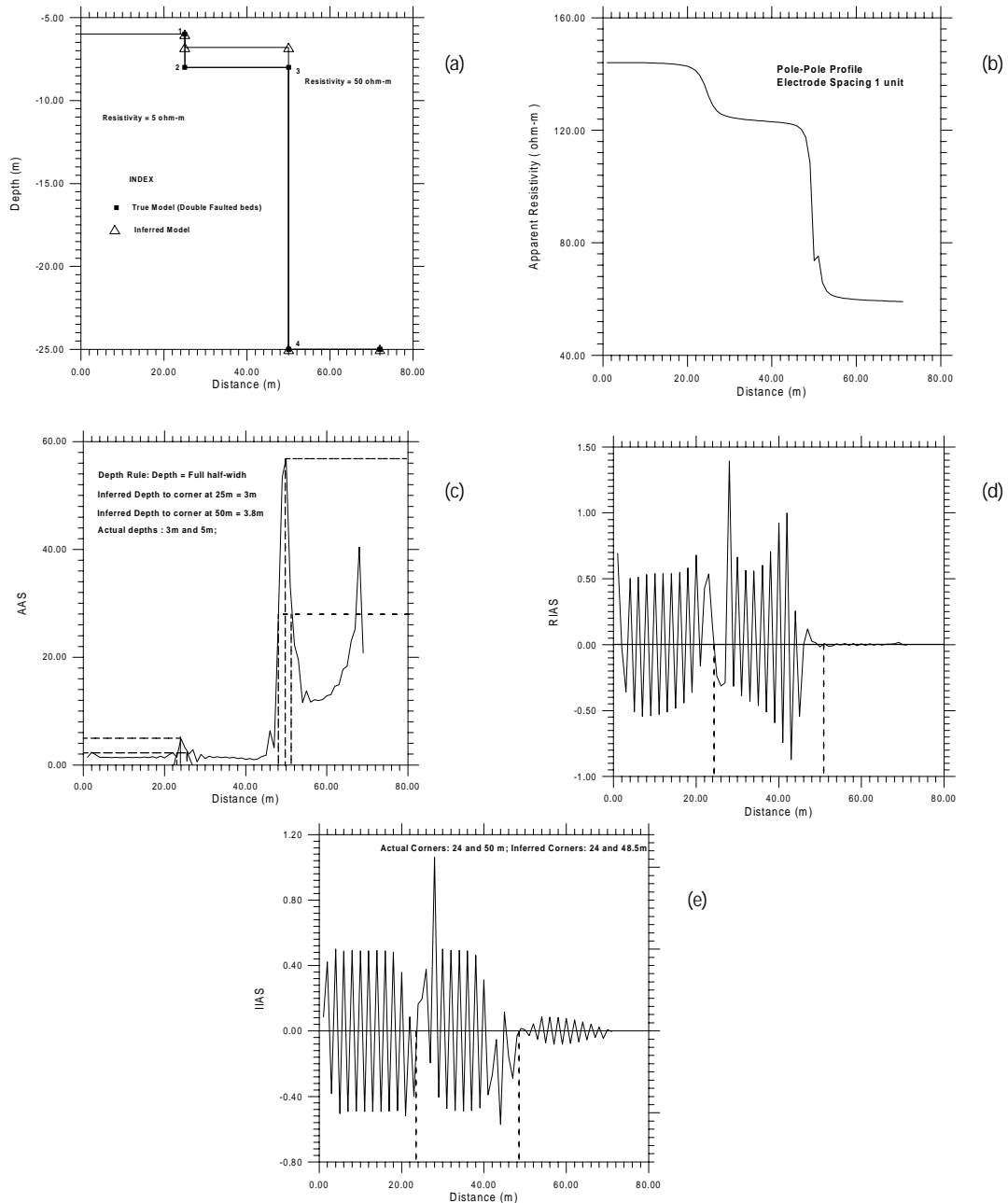


Figure 5a). Faulted bed model with corners 1, 2, 3 and 4, whose true coordinates (meters) are respectively 1(24, 6), 2(24, 8), 3(50, 8) and 4(50, 28). The buried pole-pole configuration of spacing 1m traverses across the body at 3m depth below air-earth interface along a principal profile. All inferred depth parameters by RESAS refer to depth level of pole-pole configuration. Inferred model is also displayed here. Depths are indicated with negative values. b) Pole-Pole (Half-Wenner) apparent resistivity profile for fault model (Fig. 5a) with a buried pole-pole configuration at 3m below air-earth interface. c) Amplitude of Analytic Signal (AAS) profile for fault (Fig. 5a) model. Inferred coordinates (meters) for corners 1, 2, 3 and 4 of fault model (Fig. 5a) are respectively 1(24, 3), 2(24, 3.8), 3(50, 3.8) and 4(50, -) against true coordinates 1(24, 3), 2(24, 5), 3(50, 5) and 4(50, 25). The depth of corner 4 could not be inferred separately due to superposition of analytic signals. d) Real component of complex inverse Analytic Signal (RIAS) profile for Fault model (Fig. 5a). Inferred lateral coordinates of fault corners 1, 2, 3, and 4 are respectively 24m, 24m, 51m and 51m as against true ones 24m, 24m, 50m and 50m. e) Imaginary component of complex inverse Analytic Signal (IIAS) profile for Fault (Fig. 5a). Inferred lateral coordinates of fault corners 1, 2, 3, and 4 are respectively 23.8m, 23.8m, 49m and 49m as against true ones 24m, 24m, 50m and 50m.

Table 4. Results of Stabilized Analytic Signal (RESAS) Algorithm for Fault Model (Fig. 5a)

Estimation of Lateral and depth* coordinates (X, Z) of body corners.				
Body Corner	RIAS (X- Coordinate) (m.)	IIAS (X- Coordinate) (m.)	AAS ((X, Z) oordinates) (m.)	Actual Coordinates of Body corners ((X, Z) Coordinates) (m.)
Fig. 5a	Fig. 5d	Fig. 5e	Fig. 5c	Fig. 5a
1	24	23.8	(24,3)	(24,3)
2	24	3.8	(24,3.8)	(24,5)
3	51	49	(50,3.8)	(50,5)
4	51	49	(50, -)	(50,25)

\* Depth estimates refer to depths of body corners below electrode configuration level. Buried pole-pole- configuration is 3m below air-earth interface. Pole – Pole electrode spacing is 1m.

Table 5. Results for Horst - Graben Model (Figs. 6a, 6f)

Interpretation using RESAS Estimation of Lateral and depth* coordinates (X, Z) of body corners.				
Body Corner	RIAS (X- Coordinate) (m.)	IIAS (X- Coordinate) (m.)	AAS ((X, Z) Coordinates) (m.)	Actual Coordinates of body corners ((X, Z) Coordinates) (m.)
Fig. 6a	Fig. 6d	Fig. 6e	Fig. 6c	(Fig. 6a)
1	17.5	18	(17.5,3)	(17,3)
2	26.5	26	(27.5,3)	(27,3)
3	42	46.5	(46.5,4)	(46,5)
4	58	58	(58.5,4)	(58,5)

\* Depth estimates refer to depths of body corners below electrode configuration level. Buried pole-pole- configuration is 3m below air-earth interface. Pole – Pole electrode spacing is 1m.

Secondary potential (Fig.4a) is determined by rectifying the effect of host medium, and the principle profile is plotted across the strike of body.

Secondary potential data is used as an input for RESAS. The resulting AAS (Fig. 4b) and RIAS (Fig. 4c) plots are utilized to locate body corners of input model.

Inferred model is shown in Fig. 4d and Table 3 enlists the results.

**OPEN BODIES**

Apparent resistivity profile for pole-pole and pole-dipole serve as input data to our RESAS.

**Fault Model**

A fault model is displayed in Fig.5a. Synthetic Pole-pole apparent resistivity profile is determined at a depth of 3mbelow air-earth interface for electrode spacing 1m. AAS (Fig. 5c), RIAS (Fig. 5d), and IIAS (Fig.5e) plots infer fault parameters. The results of RIAS, IIAS and AAS are given in Table 4 and in Fig. 5f.

**Horst - Graben Structure**

This model is shown in Fig.6a and its synthetic pole-pole response for buried pole-pole configuration (1m

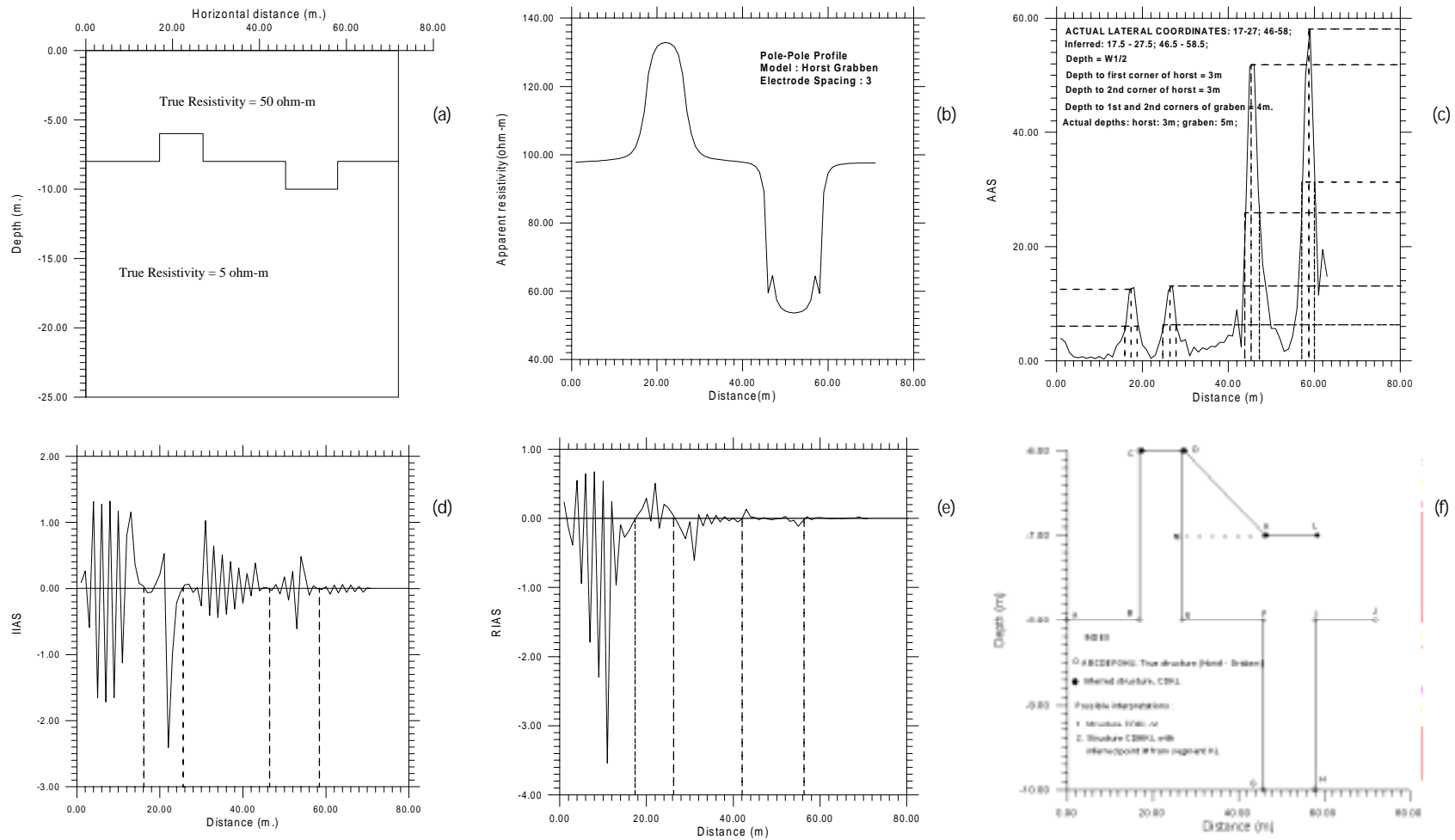


Figure 6. a) A horst – graben model. The resistivity of overlying medium is 50 ohm-m and that of substratum is 5 ohm-m. The buried Pole-Pole electrode configuration (1m electrode separation) located at 3m depth below air-earth interface traverses across the body. Depths are indicated with negative values. b) Pole-Pole (Half-Wenner) apparent resistivity profile for Horst – Graben Model (Fig. 6a). c) Amplitude of Analytic Signal (AAS) profile for horst – graben model (Fig. 6a). Both actual and inferred model parameters are included. d) Real component of complex inverse Analytic Signal (RIAS) profile for horst – graben model (Fig. 6a). RIAS zero crossings infer the lateral edges of the model. The inferred lateral coordinates for horst are 17.5 m and 26.5m and for graben are 42m and 58m. Actual lateral coordinates for horst and graben (Fig. 6a) are 17, 27, 46 and 58m respectively. e) Imaginary component of complex inverse Analytic Signal (IIAS) profile for horst – graben model (Fig. 6a). IIAS zero crossings also infer the lateral edges of the model. The inferred lateral coordinates for horst are 18 m and 26m and for graben are 46.5m and 58m. Actual lateral coordinates for horst and graben (Fig. 6a) are 17, 27, 46 and 58m respectively. f) Interpretation result for horst – graben model (Fig. 6a). Both actual (open circles) and inferred (filled-in circles) models are presented. Due to superposition of lower corners' analytic signals, only top corners of horst (C and D) and graben (K and L) could be inferred. The segments (DK and MK) could be two possible interpretations arising out of analysis. Depths are indicated with negative values.

electrode spacing) at 3m below air-earth interface is displayed in Fig. 6b. The RESAS output results are AAS (Fig.6c), RIAS (Fig.6d) and IIAS (Fig.6e) plots. The interpretation results are included in Fig.6f and Table 5. Ambiguity in interpretation due to coincident lateral coordinates of corners is illustrated.

## DISCUSSION

The numerical experiments proved that AAS can reliably be used for assessing the geometric parameters of conductive / resistive targets of both open and closed geometry. In case AAS fails to infer a body corner, e.g., corner 8 of Dyke 2 in Figs. 4b and 4d, RIAS estimate could be resorted to fix the x-coordinate of corner position and for depth, one may assume it to be same as that of corner 7. This uncertainty in corner location by AAS is due to limited input profile length. Depth estimation for bodies of open geometry is still an open question. We have empirically adopted  $2x_{1/2}$  to be the depth rule for bodies of open geometry. However, this needs further rigorous testing by more models of complex geometry.

For coincident lateral coordinates of two corners of a body (either of open or closed geometry), due to superposition of analytic signals, AAS fails to assign proper depth value for deeper corner, e.g., Fault model (Figs 5c and 5e) and Horst – Graben model (Figs 6c and 6f). This aspect is the lacunae of the analytic signal approach. In such cases, interpretation is ambiguous, e.g., In Fig. 6f, both segments represented by broken lines fail to represent the reality. So, an interpreter has to utilize other independent means to check the interpretation.

In RIAS (Figs 1d, 3c, 4c, 5d, 6d) and IIAS plots (Figs.5e,6e), we notice clear zero crossings associated with body corners attended by noisy appearance on either side. Such a behavior of RIAS or IIAS is reasonable as per potential field theory for the body corners irrespective of open or closed geometry source constitute singularities of potential.

## SUMMARY AND CONCLUSIONS

Tikhonov's regularization based stable analytic signal algorithm has provided first order guess models for input error-free pole-pole potential data in case of conductive bodies of closed geometry and resistivity data for conductive structures of open geometry. While secondary pole-pole potential data due to closed 2-D bodies formed the input data to our RESAS for open 2D bodies pole-pole resistivity profiles suffice.

Generally, AAS meets the interpretation requirements; but analysis of RIAS and IIAS is needed

either to confirm the lateral coordinates inferred by AAS or supplement such information.

In case of body corners with same lateral coordinates (bodies with vertical dips), analytical signal method fails in segregating them and ambiguity arises.

Profiles of sufficient length are needed to image the lower corners of anomaly causative sources. Numerical experiments demonstrate the use of the proposed method.

## ACKNOWLEDGEMENTS

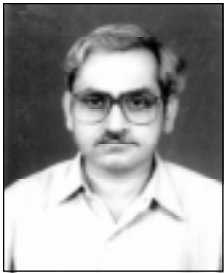
Authors convey their sincere thanks to Dr. V.N.Singh, Professor and Head, Department of Earth Sciences, IIT, Roorkee for the facilities extended to them.

## REFERENCES

- Dey, A., 1976. Resistivity modelling for arbitrary shaped two-dimensional structure, part II: User's guide to the FORTRAN algorithm RESIS2D, Laurence Berkley Lab. Rep., LBL-5283.
- Dey, A. & Morrison, H. F., 1979. Resistivity modelling for arbitrary shaped two dimensional structures, *Geophysical Prospecting*, 22, 106-130.
- Eskola, L., 1992. *Geophysical interpretation using integral equations*, Chapman & Hall, Madras, 191pp.
- Li, Y. & Oldenburg, D.W., 1991. Aspects of charge accumulation in DC resistivity experiments, *Geophysical Prospecting*, 39, 803-826.
- Li, Y., & Oldenburg, D.W., 1994. Inversion of 3-D DC resistivity data using an approximate inverse mapping, *Geophys. J. Int.*, 116, 527-537.
- Loke, M. H. & Baker, R. D., 1995. Least square decomposition of apparent resistivity pseudosections, *Geophysics*, 60 (6), 1682-1690.
- Mukesh Gupta., 2004. 2-D Geoelectric modeling and inversion, M.Tech Thesis (Unpublished), IIT, Roorkee, pp. 107.
- Nabighian, M. N., 1972. The analytic signal of two dimensional magnetic bodies with polygonal cross sections: Its properties and use for automated anomaly interpretations, *Geophysics*, 37 (3), 803-826.
- Ofoegbu, C.O. & Mohan, N.L., 1990. Interpretation of aero-magnetic anomalies over part of southeastern Nigeria using three-dimensional Hilbert Transformation, *Pageoph*, 134, 13-29.
- Press, W.H., Teukolsky, S.A., Vetterling, W.T. & Flannery, B.P., 1994. *Numerical recipes in FORTRAN*, Cambridge Univ. Press, Sanat Publishers, Delhi, 963 pp.
- Pujari, P.R., 1998. Stabilized analytic signal algorithm

- in 2D and 3D DC resistivity data analysis, Ph. D. Thesis, University of Roorkee.
- Pujari, P. R. & Sastry, R. G., 2003. 2D Stabilized analytical signal method in DC pole-pole potential data interpretation, *Indian Acad. Sci. (Earth Planet. Sci.)*, 112 (1), 37-49.
- Quick, D.H., 1974. The interpretation of gradient array chargeability anomalies, *Geophysical Prospecting*, 22, 736-746.
- Rao, A.D., Ram Babu, H.V. & Shankar Narayan, P.V., 1981. The complex gradient method, *Geophysics*, 86, 1572-1578.
- Roest, W R, Verhoef, J. & Pilkington, M., 1992. Magnetic interpretation using 3-D analytic signal, *Geophysics*, 57, 116-125.
- Sastry, R.G., & Pujari, P.R., 1997. Stabilized analytical signal method in electrical resistivity tomography, In: *Extended Abstracts book, 59<sup>th</sup> EAGE Conference and Technical Exhibition, 26-30 May 1997, Geneva, Switzerland*, P135
- Sunderrajan, N., Srinivasa Rao, P. & Sunitha, V., 1998. An analytical method to interpret self-potential anomalies caused by 2-D inclined sheets, *Geophysics*, 63, 1551-1555.
- Tikhonov, A.N. & Arsenin, V.Ya., 1977. *Solution of ill-posed problems*, John Wiley, Washington.

(Accepted 2005 June 24. Received 2005 May 13; in original form 2004 March 28)



Dr. Rambhatla G. Sastry has obtained M.Sc(Tech.) degree in Applied Geophysics from Andhra University in July 1973 and Ph.D. degree in Geophysics from Moscow State University, USSR in April 1980. He has served as CSIR Pool Officer at NGRI during 1980-81 and joined the geophysics faculty of Department of Earth Sciences, University of Roorkee during May 1981. Currently he is serving as Associate Professor in Geophysics at IIT, Roorkee. He was Commonwealth Academic Staff Fellow for the year 1989 at Geophysics Department, University of Edinburgh, Edinburgh (U.K.). His research interests include Exploration Geophysics, Geophysical Inversion and Hydrological Modelling.